

# Non-equilibrium vertex correction: disorder scattering in magnetic tunnel junctions

Youqi Ke<sup>1</sup>, Ke Xia<sup>2</sup> and Hong Guo<sup>1</sup>

<sup>1</sup> *Centre for the Physics of Materials and Department of Physics,  
McGill University, Montreal, PQ, H3A 2T8, Canada*

<sup>2</sup> *State Key Laboratory for Surface Physics, Institute of Physics,  
Chinese Academy of Sciences, P.O. Box 603, Beijing 100080, China*

(Dated: October 31, 2018)

We report a first principles formalism and its numerical implementation for treating quantum transport properties of nanoelectronic devices with atomistic disorder. We developed a nonequilibrium vertex correction (NVC) theory to handle the configurational average of random disorder at the density matrix level so that disorder effects to nonlinear and nonequilibrium quantum transport can be calculated from atomic first principles in a self-consistent and efficient manner. We implemented the NVC into a Keldysh non-equilibrium Green's function (NEGF) based density functional theory (DFT) and applied the NEGF-DFT-NVC formalism to magnetic tunnel junctions with interface roughness disorder. Our results show that disorder has dramatic effects to nonlinear spin injection and tunnel magneto-resistance ratio.

PACS numbers: 85.35.-p, 72.25.Mk, 73.63.Rt, 75.47.De

Quantitative understanding of impurity effects is crucial for nanoelectronics where device properties are strongly influenced by or even built on such effects. Examples are electron scattering by dopants in semiconductor nanowires[1] and field effect transistors, spin scattering by disorder in magnetic tunnel junctions[2], and transport of spin polarised current in dilute magnetic semiconductors[3]. Unintentional impurities sit inside a device at unpredictable locations and therefore, any physical quantity predicted by theory should be averaged over impurity configurations. In *ab initio* calculations, one may carry out this average by generating many impurity configurations for a given concentration  $x$ , calculating the relevant physical quantity for each configuration, and finally averaging the results. Such a brute force calculation is often not practical for at least two reasons. First, when  $x$  is small as is typical in the case of semiconductor devices, say 0.1%, one would need a thousand host atoms to accommodate just one impurity atom. Second, it is known that impurity average may require huge number of configurations[4]. These requirements make a calculation prohibitively large. Considerable effort has therefore been devoted in literature to develop approximate techniques which avoid brute force. In this regard, a widely used technique is the coherent potential approximation (CPA)[5] as implemented in KKR[6] and LMTO[7] first principles methods. So far CPA has been applied to *equilibrium* electronic structure and transport calculations[8]. However, most nanoelectronic devices operate under *nonequilibrium* conditions, for instance one wishes to predict nonlinear current-voltage (I-V) characteristics. It is thus very important to develop appropriate nonequilibrium techniques for impurity averaging.

Here we report our solution of the atomistic *nonequilibrium* impurity average problem for quantum transport. We start from a state-of-the-art real space atomistic

quantum transport formalism where density functional theory (DFT) is carried out within the Keldysh nonequilibrium Green's function (NEGF) framework[9, 10]. The basic idea of NEGF-DFT is that the device Hamiltonian and electronic structure are determined by DFT, the nonequilibrium quantum statistics of the device physics is determined by NEGF, and the transport boundary conditions under external bias are handled by real space numerical technique. We deal with impurity average at single particle retarded Green's function level by CPA[5], and at NEGF level by evaluating a nonequilibrium vertex correction (NVC) term. The NEGF-DFT-NVC formalism allows us to construct *nonequilibrium density matrix* self-consistently that includes impurity averaging. We then apply our NEGF-DFT-NVC formalism to investigate effects of interface roughness disorder in a magnetic tunnel junction (MTJ). Our results indicate that disorder effect can drastically and qualitatively influence nonlinear I-V curves and tunnel magneto-resistance ratio.

We consider a two-probe device consisting of a scattering region and two semi-infinite leads extending along the transport direction  $\mathbf{z}$  to  $z = \pm\infty$ , as shown in Fig.1. The system is periodically extended along the transverse (x,y) direction. Note the scattering region includes several layers of lead atoms[9]. A bias voltage  $V_b$  is applied across the leads to drive a current flow, *i.e.*  $\mu_l - \mu_r = eV_b$  where  $\mu_{l,r}$  are electrochemical potentials of the left/right leads. We assume that impurities exist inside the scattering region randomly but not in the leads. We further assume that any atomic position  $R$  in the scattering region may be occupied by two atomic species, the host and impurity atoms labelled by  $Q = A, B$  with concentrations  $C_R^A$  and  $C_R^B$  such that  $C_R^A + C_R^B = 1$ .

In a NEGF-DFT self-consistent analysis[9] of *ordered* systems, the non-equilibrium density matrix is calculated by NEGF  $\mathbf{G}^<(E)$ , *i.e.*  $\hat{n}(E) \sim \mathbf{G}^<(E)$ , here  $\mathbf{G}^<$  satisfies the Keldysh equation  $\mathbf{G}^< = \mathbf{G}^R \Sigma^< \mathbf{G}^A$

where  $G^{\mathcal{R}} = (G^{\mathcal{A}})^{\dagger}$  is the retarded Green's function.  $\Sigma^{<} = i\Gamma_l f_l + i\Gamma_r f_r$  is the lesser self-energy where  $f_{l,r}$  are Fermi functions of the left/right leads;  $\Gamma_{l,r}$  are line-width functions describing coupling of the scattering region to the leads and they can be calculated by standard iterative methods[9]. Translational invariance of ordered system allows one to evaluate all quantities in the unit cell by integration over two dimensional (2D) Brillouin zone (BZ) in the (x,y) direction. When there are impurities, translational symmetry is broken. The spirit of CPA is to construct an effective medium theory by an impurity configurational average that restores the translational invariance. For NEGF this means calculating  $\overline{G^{<}} = \overline{G^{\mathcal{R}}\Sigma^{<}G^{\mathcal{A}}}$ . Even though there is no impurity in the leads to affect  $\Sigma^{<}$ , the impurity average  $\overline{(\dots)}$  correlates Green's functions  $G^{\mathcal{R}}$  with  $G^{\mathcal{A}}$ . In particular,  $\overline{G^{<}} \neq \overline{G^{\mathcal{R}}}\Sigma^{<}\overline{G^{\mathcal{A}}}$  due to multiple scattering by the impurities. To calculate  $\overline{G^{<}}$ , we introduce a self-energy  $\Gamma_{NVC}$  that is a consequence of impurity scattering at *nonequilibrium*, such that  $\overline{G^{<}} = \overline{G^{\mathcal{R}}(\Sigma^{<} + \Gamma_{NVC})G^{\mathcal{A}}}$ .  $\Gamma_{NVC}$  is called *nonequilibrium vertex correction* (NVC) whose equilibrium counterpart is well known in calculations of Kubo formula by Feynman diagrammatic techniques[11]. There is however a major qualitative difference here:  $\Gamma_{NVC}$  depends on the non-equilibrium quantum statistical information of the device scattering region while the equilibrium VC does not.

We found that  $\Gamma_{NVC}$  is most conveniently calculable using a *site* oriented calculation scheme, for this reason we develop our NEGF-NVC theory within TB-LMTO DFT implementation[12], using CPA [7, 8] to describe the averaged system. In this approach, impurity average for any single site physical quantity  $X_R$  is given by

$$\overline{X_R} = \sum_{Q=A,B} C_R^Q \overline{X_R^Q} \quad (1)$$

where  $\overline{X_R^Q}$  is the conditional average over a particular atomic specie  $Q$  at site  $R$  which is calculated by

$$\overline{X_R^Q} = \overline{\eta_R^Q X_R / C_R^Q}. \quad (2)$$

Here  $\eta_R^Q$  is the occupation of site  $R$  by atomic specie  $Q$  and its average is  $\overline{\eta_R^Q} = C_R^Q$ . Eq.(1) means the average of a quantity at site  $R$  is a linear combination of contributions from each atomic species.

The technical derivation details are given in the Supplemental Material associated with this paper[13], here we briefly outline the spirit of the theory. The impurity average of the site diagonal NEGF is carried out by application of Eq.(1), *i.e.*  $\overline{G_{RR}^{<}} = \sum_{Q=A,B} C_R^Q \overline{G_{RR}^{<,Q}}$ . The *atom*

*resolved* NEGF  $\overline{G_{RR}^{<,Q}}$  gives atom resolved average local charge density  $\overline{n_R^Q} \sim \overline{G_{RR}^{<,Q}}$  which is needed in the DFT self-consistent iterations[9]. To find  $\overline{G_{RR}^{<,Q}}$ , we use Eq.(2).

The final expressions of  $\overline{G_{RR}^{<,Q}}$  are given in Eqs.(10,28,29) of the Supplemental Material[13], and it is related to  $\Gamma_{NVC}$  of the auxiliary NEGF. The calculation of NVC is carried out by application of single-site approximation (SSA) within CPA-based multiple scattering theory as summarised in Supplemental Material[13] where the final expression is given by Eq.(23) there. From  $\Gamma_{NVC}$  we obtain  $\overline{G_{RR}^{<,Q}}$  hence the averaged density matrix  $\overline{n_R^Q}$  for atom  $Q$  on site  $R$ . The charge density is used to calculate device Hamiltonian for the next step in the DFT iteration and this procedure is repeated until numerical convergence.

An extremely stringent test of our NEGF-DFT-NVC formalism and its numerical implementation is carried out by calculating two-probe devices at *equilibrium*, and check if the fluctuation-dissipation relationship is satisfied or not. Mathematically, fluctuation-dissipation theorem dictates  $\overline{G_{RR}^{<,Q}} = \overline{G_{RR}^{\mathcal{A},Q}} - \overline{G_{RR}^{\mathcal{R},Q}}$  at *equilibrium*. Here, calculation of  $\overline{G_{RR}^{<,Q}}$  requires NVC while calculations of  $\overline{G_{RR}^{\mathcal{A},Q}}$  and  $\overline{G_{RR}^{\mathcal{R},Q}}$  do not. For many disordered device structures including that in Fig.1 we have checked, the fluctuation-dissipation relationship is always satisfied to at least one part in a million and the final tiny difference can be attributed to numerical calculation issues. Importantly, we found that NVC is extremely important: without it the density matrix and transmission coefficients can have large errors and even become qualitatively incorrect.

After the NEGF-DFT-NVC self-consistent calculation is converged we calculate current-voltage (I-V) characteristics by Landauer formula, where an additional vertex correction must be done on the transmission coefficients[16]. At low temperature the I-V curve is given by:

$$\overline{I} = \frac{e}{h} \int_{\mu_r}^{\mu_l} Tr \left[ \overline{\Gamma_l g^{\mathcal{R}} \Gamma_r g^{\mathcal{A}}} \right] dE. \quad (3)$$

The integrand of the above expression is the transmission coefficient where the impurity average, once again, correlates the retarded  $g^{\mathcal{R}}$  and advanced  $g^{\mathcal{A}}$  Green's functions ( $g^{\mathcal{R},\mathcal{A}}$  are auxiliary Green's functions of  $G^{\mathcal{R},\mathcal{A}}$ , see Supplemental Material) connected by line-widths  $\Gamma_{l,r}$  corresponding to the auxiliary  $g$ . We write the averaged transmission into a coherent part and a vertex part which describes the inter-channel scattering events:

$$\overline{T} = Tr \left[ \Gamma_l \overline{g^{\mathcal{R}}} \Gamma_r \overline{g^{\mathcal{A}}} \right] + Tr \left[ \Gamma_l \overline{g^{\mathcal{R}}} \Gamma'_{VC} \overline{g^{\mathcal{A}}} \right] \quad (4)$$

where  $\Gamma'_{VC,R}$  is obtained from the expression of  $\Gamma_{NVC}$  by replacing  $\Sigma^{<}$  with  $\Gamma_r$ . The equilibrium conductance for a spin channel is given by  $\overline{T}(e^2/h)$ .

As an important application of the NEGF-DFT-NVC formalism, we have investigated a disordered MTJ shown in Fig.1 which consists a vacuum (Vac) tunnel barrier sandwiched by two Fe leads. The *Fe/Vac* interface has

roughness disorder which substantially influences spin dependent transport at equilibrium[17]. Here we focus on nonequilibrium. In our Fe/Vac/Fe MTJ, the left/right Fe/Vac interface layers has  $x\%$  and  $(1-x)\%$  Fe atoms respectively, and the rest are vacuum sites. The scattering region consists of ten perfect atomic layers of Fe oriented along (100) on the left and right ending with the rough interface sandwiching four vacuum layers. The scattering region is connected to perfect Fe left/right leads extending to  $z = \pm\infty$ . Because the entire structure, after impurity average, is periodic along the transverse  $x, y$  directions, we found that very careful two-dimensional Brillouin zone (BZ) sampling is necessary in calculating the density matrix: we use  $200 \times 200$  k-mesh to ensure excellent numerical convergence. For the I-V curve calculation, Eq.(3),  $300 \times 300$  BZ k-mesh is used for each point in the energy integration. For other DFT details we follow standard TB-LMTO literature[17].

Fig.2a is a semi-log plot of equilibrium ( $V_b = 0$ ) conductance versus disorder  $x$  for both spin-up and -down channels,  $G_\uparrow, G_\downarrow$ . The four curves correspond to magnetic moments of the two Fe leads having parallel or anti-parallel configurations (PC or APC). Since the left interface is chosen to be  $Fe_xVac_{1-x}$  while the right  $Fe_{1-x}Vac_x$ ,  $G_{\uparrow,\downarrow}$  are both symmetric about  $x = 0.5$  in PC (black squares and red circles). For APC they are not symmetric but satisfy  $G_\uparrow(x) = G_\downarrow(1-x)$ , as expected. Impurity scattering dramatically decreases  $G_\downarrow$  in PC, and has relatively less effect for  $G_\uparrow$  and for APC. It was well known[18] that for perfect interfaces, the surface electronic states of Fe give resonance transmission. These resonances are destroyed rapidly by the interface disorder as  $x$  changes from zero to 50% leading to the drastic reduction of  $G_\downarrow$  in PC. An important device merit for MTJ is the tunnel magneto-resistance ratio (TMR) defined by total tunnelling currents for PC and APC:  $TMR = (I^{PC} - I^{APC})/I^{APC}$ . At equilibrium when all currents vanish, we use equilibrium conductances to calculate TMR. Fig.2b plots equilibrium TMR versus  $x$  showing a dramatic effect of disorder. In particular, TMR drops to very small values, even to slightly negative values, as  $x$  is increased from zero. These equilibrium features are consistent with previous super-cell calculations[17].

We now investigate nonequilibrium properties when  $V_b \neq 0$  so that current flows through. To show the importance of NVC, we have calculated I-V curves at  $x = 0.05$  by including vertex correction only at the level of transmission coefficient, *i.e.* without NVC in the NEGF-DFT self-consistent iterations of the density matrix: the solid lines (green) in Fig.3a plot this result. In comparison, the dashed lines (red) plot the full results where NVC is included. The substantial differences indicate that NVC is extremely important for obtaining correct results at nonequilibrium. Fig.3b and its inset plot TMR versus bias for four values of  $x = 0.0, 0.05, 0.3, 0.5$ , obtained by

the full NVC formalism. For zero or small values of  $x$ , TMR reduces with  $V_b$  as is often seen in experimental measurements[19]. For larger  $x$ , for instance  $x \sim 0.5$ , TMR can go negative as  $V_b$  is increased. Indeed, experimental measurements had seen[20] negative TMR at large  $V_b$ , although for different MTJs and possibly different physical origin. Very dramatically, at  $x = 0.3$ , the entire TMR curve is negative: here the absolute value of TMR actually increases with  $V_b$  (see inset). These behaviours of TMR strongly suggest that interface disorder play very important roles for nonequilibrium spin injection.

Fig.4 plots spin currents and TMR versus disorder  $x$  at  $V_b = 0.544V$ . This is to be compared with Fig.2 where  $V_b = 0$ . A finite bias breaks left-right symmetry of the atomic structure and therefore, the spin currents do not have a symmetric behaviour about  $x = 0.5$  anymore. Both spin currents (Fig.4a) and TMR (Fig.4b) varies with disorder  $x$  in substantial ways. In particular, TMR rapidly dips to negative values when  $x$  is increased to about 20%. So far we have focused on devices where the left has a  $Fe_xVac_{1-x}$  interface while the right has  $Fe_{1-x}Vac_x$ . We have also applied the NEGF-DFT-NVC formalism to devices where the left and right interfaces are disordered totally differently. The inset of Fig.4b plots TMR for such a system where left interface has  $x = 0.3$  while the right interface has  $x = 0.05$ . For this system TMR is negative and its absolute value decreases as  $V_b$  is increased which is qualitatively similar to what discussed above.

In summary, we have developed a nonequilibrium vertex correction theory and its associated software for analysing quantum transport properties of disordered nanoelectronic devices at nonequilibrium. The impurity averaging of the nonequilibrium density matrix is facilitated by the NVC self-energy that is related to quantum statistical information of the device scattering region. Our NEGF-DFT-NVC theory has several desired features, including atomistic first principle, non-equilibrium, efficient configurational average and self-consistency. This allows us to analyse nonequilibrium quantum transport of realistic device structures including realistic atomic substitutional impurities. Using this tool, we have calculated nonlinear spin currents in Fe/Vac/Fe MTJ with interface roughness disorder, and found that effects of NVC can play a dominant role in determining the properties of spin injection.

**Acknowledgements.** We gratefully acknowledge useful discussions with Zhanyu Ning, Wei Ji, Dr. Lei Liu and Dr. Eric Zhu. This work is supported by NSERC of Canada, FQRNT of Quebec and CIFAR (H.G.). K.X. is supported by NSF-China (10634070) and MOST (2006CB933000, 2006AA03Z402) of China. We are grateful to RQCHP for providing computation facility.

- 
- [1] T. Markussen, R. Rurali, A.P. Jauho and M. Brandbyge, Phys. Rev. Lett. **99**, 076803 (2007).
- [2] A. M. Bratkovsky, Phys. Rev. B. **56**, 2344 (1997); E.Y. Tsymbal, A. Sokolov, I.F. Sabirianov and B. Doudin, Phys. Rev. Lett. **90**, 186602 (2003).
- [3] H. Ohno, Science, **281**, 951 (1998).
- [4] W. Ren, Z. Qiao, J. Wang, Q. Sun, and H. Guo, Phys. Rev. Lett. **97**, 066603(2006).
- [5] P. Soven, Phys. Rev. **156**, 809 (1966); B. Velický S. Kirkpatrick and H. Ehrenreich, Phys. Rev. **175**, 747 (1968).
- [6] W.M. Temmerman, B.L. Gyorffy and G.M. Stocks, J. Phys. F **8**, 2461 (1978); G.M. Stocks and H. Winter, Z. Phys. B **46**, 95 (1982); N. Stefanou, R. Zeller and P.H. Dederichs, Solid State Commun. **62**, 735 (1987).
- [7] I. Turek *et al.* *Electronic Structure of the Disordered Alloys, Surfaces and Interfaces*, (Kluwer, Boston, 1997); J. Kudrnovský and V. Drchal, Phys. Rev. B **41**, 7515 (1990); J. Kudrnovský, V. Drchal and J. Masek, Phys. Rev. B **35**, 2487 (1987).
- [8] K. Carva, I. Turek, J. Kudrnovský and O. Bengone, Phys. Rev. B **73**, 144421 (2006).
- [9] J. Taylor, H. Guo and J. Wang, Phys. Rev. B **63**, 121104(R) (2001); *ibid* **63**, 245407 (2001); D. Waldron, P. Haney, B. Larade, A. MacDonald and H. Guo, Phys. Rev. Lett. **96**, 166804 (2006).
- [10] S. Datta, “Electronic Transport in Mesoscopic System”, (Cambridge University Press, 1995).
- [11] G.D. Mahan, “Many-Particle Physics”, (Plenum, New York, 1981).
- [12] O.K. Andersen and O. Jepsen, Phys. Rev. Lett **53**, 2571 (1984).
- [13] See EPAPS Document No. for detailed derivations.
- [14] S.V. Faleev, F. Leonard, D.A. Stewart and M. vanSchilfgaarde, Phys. Rev. B **71**, 195422 (2005).
- [15] B. Velický, Phys.Rev **184**, 614 (1969).
- [16] J. Kudrnovsky *et al.*, Phys. Rev. B **62**, 15084 (2000); I. Turek, J. Kudrnovsky, V. Drchal, L. Szunyogh and P. Weinberger, Phys. Rev. B **65**, 125101 (2002).
- [17] P.X. Xu *et al.*, Phys. Rev. B **73**, 180402(R) (2006).
- [18] J.A. Stroscio, D.T Pierce, A. Davies, R.J. Celotta and M. Weinert, Phys. Rev. Lett. **75**, 2960 (1995); O. Wunnicke *et al.*, Phys. Rev. B **65**, 064425(2002).
- [19] R. Jansena and J.S. Moodera, Appl. Phys. Lett. **75**, 400 (1999); S.S.P. Parkin *et al.*, Nature Materials, **3**, 862 (2004); S. Yuasa *et al.*, Nature Materials, **3**, 869 (2004).
- [20] J.S. Moodera *et al.*, Phys. Rev. Lett. **83**, 3029 (1999).

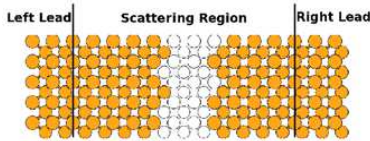


FIG. 1: (Colour online) Schematic of atomic structure of the Fe/Vac/Fe magnetic tunnel junction. The two Fe/Vac interfaces have roughness disorder. Fe: yellow spheres; vacuum: white spheres.

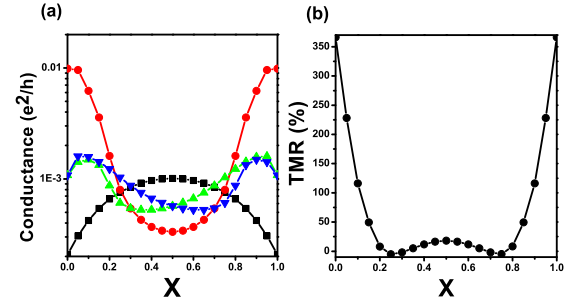


FIG. 2: (Colour online) (a) Conductance  $G_{\uparrow,\downarrow}$  versus disorder  $x$  at equilibrium. Red circles:  $G_{\downarrow}$  in PC; black squares:  $G_{\uparrow}$  in PC. Blue down-triangles:  $G_{\downarrow}$  in APC; Green up-triangles:  $G_{\uparrow}$  in APC. (b) TMR Versus  $x$ .

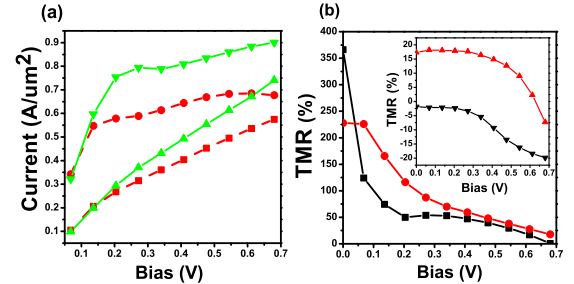


FIG. 3: (Colour online) (a) Comparison of I-V curves with disorder  $x = 0.05$ . Solid lines (green): current for PC (up-triangles) and APC (down-triangles) without using NVC in density matrix self-consistent iteration. Dashed lines (red): current for PC (circles) and APC (squares) using the full NVC formalism. (b) TMR versus bias voltage  $V_b$  for four different values of  $x$ . The main figure is for  $x=0.0$  (black squares) and  $x=0.05$  (red circles); the inset for  $x=0.3$  (black down-triangles) and  $x=0.5$  (red up-triangles)

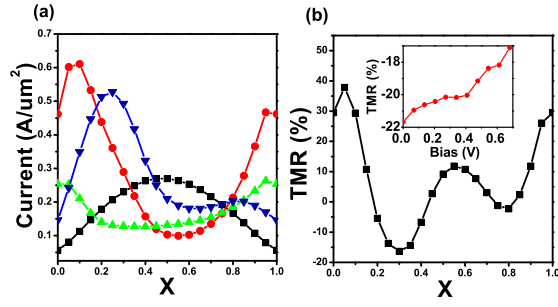


FIG. 4: (Colour online) (a) Spin currents versus disorder  $x$  at bias  $V_b = 0.544\text{V}$ , for PC and APC. Red circles and black squares: spin currents for spin-up and -down in PC; green up-triangles and blue down-triangles: spin currents for spin-up and -down in APC. (b) TMR versus  $x$  at the same  $V_b$ . Inset of (b): TMR versus  $V_b$  for a device where left and right interfaces have different values of  $x$ , on the left interface  $x = 0.3$ , on the right  $x = 0.05$ .